Available online at www.sciencedirect.com
SCIENCE DIRECT
ELSEVIER
International Journal of Machine Tools & Manufacture 46 (2006) 1811–1822
INTERNATIONAL JOURNAL OF MACHINE TOOLS & MANUFACTURE DESIGN, RESEARCH AND APPLICATION
www.elsevier.com/locate/ijmactool

An expert system for generation of machine inputs for laser-based multi-directional metal deposition

Rajeev Dwivedi, Radovan Kovacevic*

Research Center for Advanced Manufacturing, Southern Methodist University, 1500 International Parkway Suite 100 Richardson, TX 75081, USA

Received 27 September 2005; received in revised form 8 November 2005; accepted 15 November 2005
Available online 11 January 2006

Abstract

Laser-based multi-directional metal deposition (LBMDMD) is a very effective way of fabricating a part directly from its digital model. The method, however, requires a lot of human intervention during the process planning. Driven by already developed expert systems for the process planning in Computer Aided Design (CAD) and manufacturing, this paper intends to suggest a task framework for the automation of the process planning for LBMDMD using principles of *Artificial Intelligence* (AI). The process can be divided into distinct steps, and geometric reasoning can be applied to determine a set of facts and rules for the automation. The principles of first order logic are applied for the representation and further simplification of the process into a set of "if–then" based rules. This paper explains the framework, the facts, and the rule base used for the process planning.

Keywords: Expert system; Path planning; CAD; Laser-based deposition

1. Introduction

Since its conception *Artificial Intelligence* (AI) has benefited various fields. One of the implementations of the principles of AI includes the development of computer-based *expert systems* that seek to capture the human specialist's knowledge [1]. Inherent to the application of the expert system is the enhanced efficiency of the processes and lesser human intervention. Recently, the expert systems have gained a significant attention by manufacturing and material processing researchers. Some of the foremost applications of the *expert systems* in manufacturing include job scheduling and process planning [2–7]. This paper describes the application of AI to develop an *expert system* for the fabrication of a part directly from its CAD model by laser assisted multi-directional layered metal deposition.

The fabrication techniques based on the layered deposition allow an independence of the part geometry over the implementation setup. The process as shown in Fig. 1 primarily involves the slicing of the computer solid model of a part by a set of suitably spaced planes. Corresponding to each slice, a two-dimensional cross-sectional area is obtained. The metal is deposited along each such slice in a sequential manner in order to get the desired shape. This process belongs to a family of fabrication techniques referred to as Solid Freeform Fabrication (SFF).

In most of the SFF techniques, the fabrication of parts having overhanging structures relies on the support structures. The support structures are then removed in the post processing stages. The post processing of the prototype, which involves machining or chemical treatment to remove the support structures, makes the process invariably time consuming, inefficient, and involve human intervention at multiple steps. The multi-directional deposition eliminates the requirement of the support structure by suitably orienting the part during the deposition process such that a support is always provided during the deposition.

Recently, certain multi-directional material deposition [8–10] and doubled-sided layered manufacturing [11] have

*Corresponding author. Tel.: +1 214 768 4865; fax: +1 214 768 0812.
E-mail address: kovacevi@engr.smu.edu (R. Kovacevic).

0890-6955/$ - see front matter © 2005 Elsevier Ltd. All rights reserved.
doi:10.1016/j.ijmachtools.2005.11.008

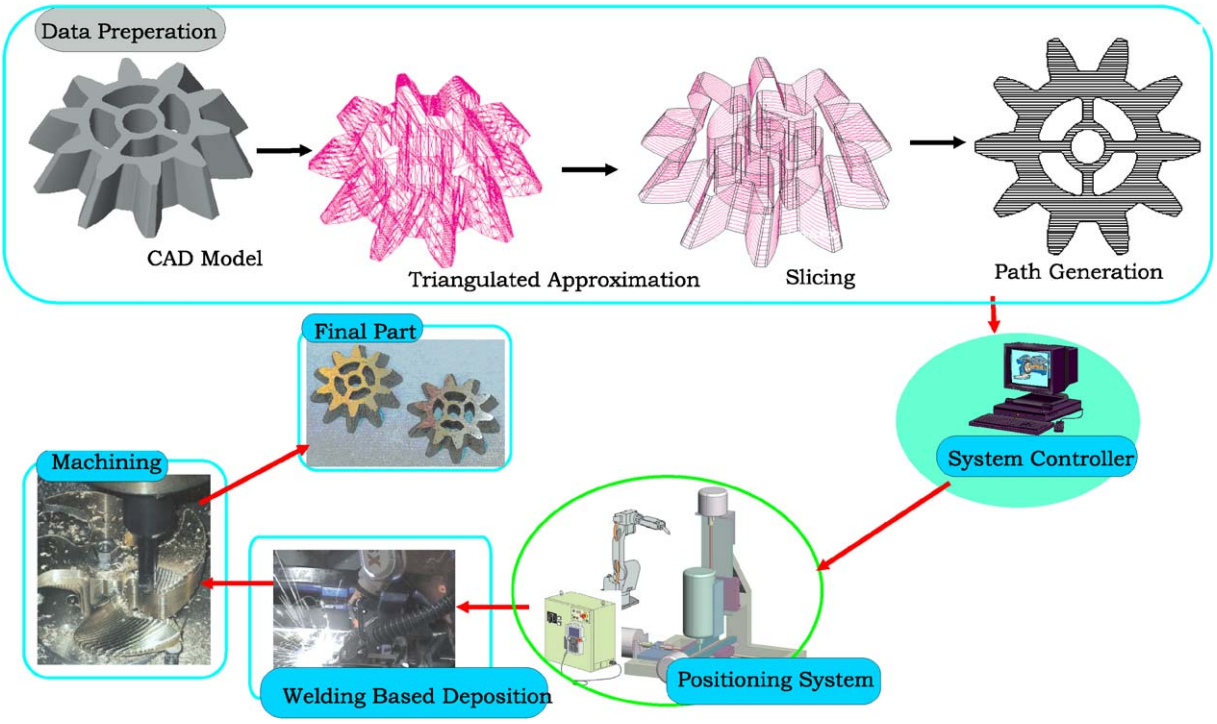

Fig. 1. The basic steps in the part fabrication by multi-axis deposition.

been suggested. However, not much has been said about the automation of the process planning. A closer observation of the proposed algorithms suggests that the primary factors involved in the decision making are guided by the geometry of the part. The framework for the development of an expert system to automate the generation of machine inputs may be divided into two groups:

1. Identification of different components of the geometry.
2. Application of geometric reasoning for the "if–then" based hierarchy of the steps of implementation.

A brief introduction to the multiple axis deposition method is explained in the sections below. Also, certain geometric preliminaries that form the basis of the process planning are explained. A more detailed account of the method is described by another paper by the authors [12]. The later sections describe, in detail, the application of AI towards the development of an expert system for the process planning. The paper concludes with the experimental results and suggestions for future direction.

2. Geometric preliminaries

This section elaborates upon two geometric notions: the *morphological skeleton* of a solid and, the *C-space* used towards the process planning and derivation of the process inputs.

2.1. Morphological skeleton of a solid

A solid S, is defined as a closed subset of Euclidean space R^3. The interior of the solid is defined as $p \in S$ and its exterior is the complement $p \notin S$. The boundary of the solid is defined by $p \in \partial S \subset S$ that is the proper subset of the solid where any neighborhood contains non-members.

The distance transform maps the solid to its equivalent distance field and the morphological skeleton of the object. The corresponding distance field [13] is the scalar field associated with solid $S, F : R^3 \to R$, that maps a point in space to the distance from that point to the closest on ∂S such that

$$F(p) = \begin{cases} -\min_{\forall Q \in \partial S}(|p - Q|), & p \in S, \\ 0, & p \in \partial S, \\ -\min_{\forall Q \in \partial S}(|p - Q|), & p \notin S. \end{cases} \quad (1)$$

A wide number of techniques such as Voronoi Graphs [14], Medial Axis Transform [15], use of Polyball Approximation [16], and Voxel arrangement [17], have been suggested for skeleton generation.

2.2. C-space

The configuration space or C-space mapping transforms the problem of planning the motion of a dimensioned object into the problem of planning the motion of a point. The formulation of the configuration space is obtained by "growing" obstacles by the shape of the moving object (Fig. 2). The space, thus obtained, simplifies to the

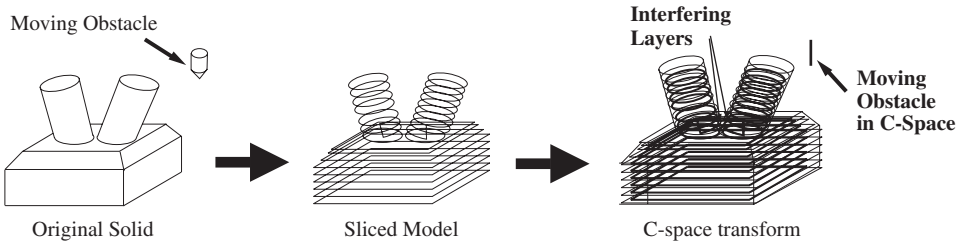

Fig. 2. Part decomposition, slicing, C-space transformation and determination of interference geodesic level.

representation of the moving object as a point. The apparent advantage of a configuration space transformation is the reduction in the number of degrees of freedom, and hence, the problem variables.

3. Fundamental steps of the process planning

Referring to Fig. 1 the basic approach of fabricating the part directly from the model includes:

Step 1: Generate the CAD model of the geometric object such that the outer surface is approximated as a set of interconnected triangles (STL format).

Step 2: Determine the overhanging regions of the solid in a given orientation and the vectors directed along the morphological skeleton of the solid, and decompose the solid into different sub-regions based on the vectors.

Step 3: Slice each of the subregions of the CAD model by a set of parallel planes oriented normal to the morphological skeleton vector of the subregion.

Step 4: Generate the C-space of the sliced model and determine the possible interferences.

Step 5: Arrange the order of the layers in a suitable order for fabrication.

Step 6: Determine the orientations for the subregions and the machine inputs for the metal deposition.

For most of the laser-based metal deposition methods, the part building is based on the sequential layered deposition of metal along a suitable growth vector to get the desired shape. In the given approach, the solid is divided into a set of sub-volumes, and the growth-vector for each sub-volume is different. A suitable decomposition and orientation of the part eliminates the requirement for the support structures, but the finite volume of the laser deposition head can cause a collision with the previously deposited layers and other components of the setup. A collision detection algorithm based on the configuration space is used to find out the possible regions of collision. Subsequently:

1. Reorient the part and the deposition vector.
2. Rearrange the sequence of the layers.
3. Use a combination of 1 and 2.

For geometrically simple parts, the reorientation of the part is sufficient in order to eliminate the support requirement; however, for a complex shape, a combination of orientation along with a suitable sequencing of the layers is required to fabricate the part. Finally, the diagnosis of any possible collision and the subsequent modification in the process is required. Another associated limitation is the possible inaccessibility of the deposition head to all the regions. In the present approach, the metal deposition is modified to a combination of a sequential and parallel layered deposition of the slices for the conflicting regions. The application of this approach is governed by the identification of the interfering regions and by the rearrangement of the order of the slices.

As described earlier, the slicing plane vector for each region is assigned based on the morphological skeleton and is different for different regions. The intersection of the plane with respect to the solid model generates a set of planar contours. The C-space is obtained by attributing the dimensions of the material deposition head to the contours. Let us define the contour in C-space as C-contours. The geometry of the metal deposition head, as described in Fig. 3 is axi-symmetric. The metal deposition head diameter varies along the z-axis and is expressed by following mathematical function:

$$r = \begin{cases} z \tan \theta(t), & z \leqslant z_1, \\ R, & z > z_1. \end{cases} \tag{2}$$

The corresponding C-contour function is obtained by attributing the geometric function of the metal deposition head to the geometry of the contours, given by following relation:

$$R_c = r \oplus R', \tag{3}$$

where R_c is the geometry of the contour of section in the C-space, that is, the C-contour, and r is the radius of the metal deposition head; whereas, R' is the boundary of the initial geometry of the contour.

Let us define a term sequence-number of a slice. The sequence-number refers to the order of the slice with respect to the base point of the subregion of a solid. Collision is detected by investigating any possible overlaps of the cross-sections of the slices. The region of interference is the common overlapping area between the planar polygonal sections oriented along multiple directions.

As described in Fig. 2, the part is decomposed into three regions and sliced along the respective growth vectors. The

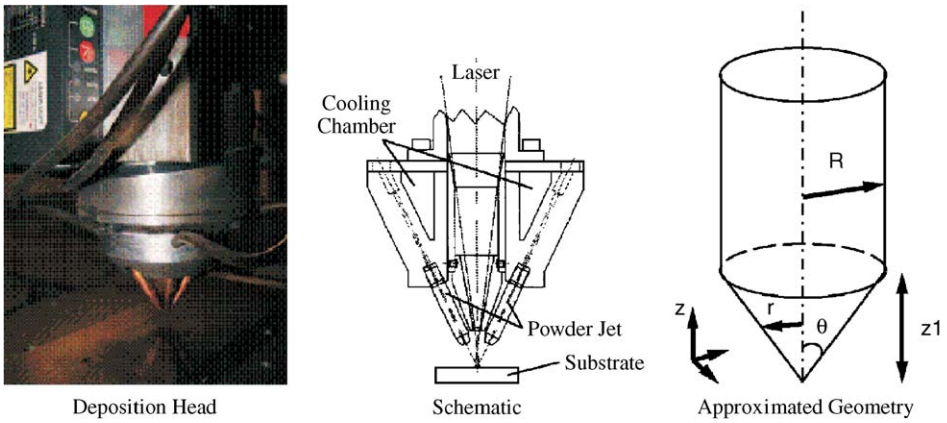

Fig. 3. The metal deposition head geometry.

C-space is obtained by expanding the initial contours through the metal deposition head dimensions. Let us define a second parameter "interference-geodesic-level", attributed to the interfering layers. Starting from the first layer, the interference-geodesic-level corresponds to the order in which the interference between two expanded layers appears.

All the contours that depict mutual interference are classified to be at the same interference-geodesic-level. Once the interference-geodesic-level for all the layers is assigned, the order of deposition is decided. The assignment of order is based on the sequence-number of the layer. However, for all the contours that are at the same level, the order is established along a given order of the sub-volumes of the solid. Fig. 4 describes the process planning for a solid divided into five sub regions $R_1, R_2, \ldots, R_5$. Let each region be sliced and modified to get the corresponding C-contours $R_1L_0, R_1L_1 \ldots$ for regions $R_1, R_2L_0, R_2L_1 \ldots$ for region R_2 and so on. The $L_0, L_1 \ldots$ are referred to as the sequence number of a slice. The interference between the layers is determined, and the corresponding interference-geodesic-level $Gd_1, Gd_2 \ldots$ is assigned to all the layers. The layers with the same interference-geodesic-level are grouped together. The deposition for all the layers at the same interference-geodesic-level, allows collision-free fabrication. However, each layer is deposited on the previously deposited layers; therefore, the feasibility of part fabrication by layered deposition is possible by following a suitable order of fabricating the layers. Fig. 4 shows the sequence of building the layers. The steps for assigning the layer order number are as follows:

Step 1: Arrange the list of layers in the order of region number.

Step 2: Prepare a master list by appending the lists for each region in the order of region number.

Step 3: Start from the first element in the master list; cluster and sort the layers with the same geodesic order together.

The final order of the layers is identified by assigning a sequence number in the order of deposition to the layers. Path generation for the metal deposition head is beyond the scope of this research; however, a detailed description of the approach is described in [18].

4. The experimental setup

The deposition is implemented using an 11-degree of freedom (DOF) manipulator that consists of a 6-axis robot and a 5-axis CNC machining center (Fig. 5) called *MultiFab* that is under development at the Research Center for Advanced Manufacturing, SMU [19]. The MultiFab system integrates a variety of metal deposition and removal techniques for the fabrication of a part directly from the CAD model. Gas Tungsten Arc Welding-based deposition and LBDMD are the primary modes of metal addition; however, this paper addresses the methodology of metal addition based on the LBDMD. A metallic substrate is mounted on a platform that can move along the X-axis and Y-axis, can tilt about a horizontal axis, and rotate about a vertical axis as shown in Fig. 5. The metal deposition head is mounted on a six-DOF robot. The relative motion of the substrate and the robot allow the fabrication of various geometries. The robot, in essence, provides the motion along the Z-axis and the orientation of the metal deposition head normal to the immediate layer.

5. First order logic for the process planning

The existing models for the process planning of the deposition of various geometries are based on deposition along only one direction; hence, the models follow very trivial principles. On the contrary, the multi-directional deposition involves many complex rules that depend on part geometry and the machine manipulatability. Fig. 6 shows the basic architecture of an expert system for the process planning of a multi-directional metal deposition. The knowledge base is comprised of two attributes, the rule attributes and fact attributes. The fact attribute is built upon the system requirements. The rule attribute, on the other hand, is built upon the process parameters and

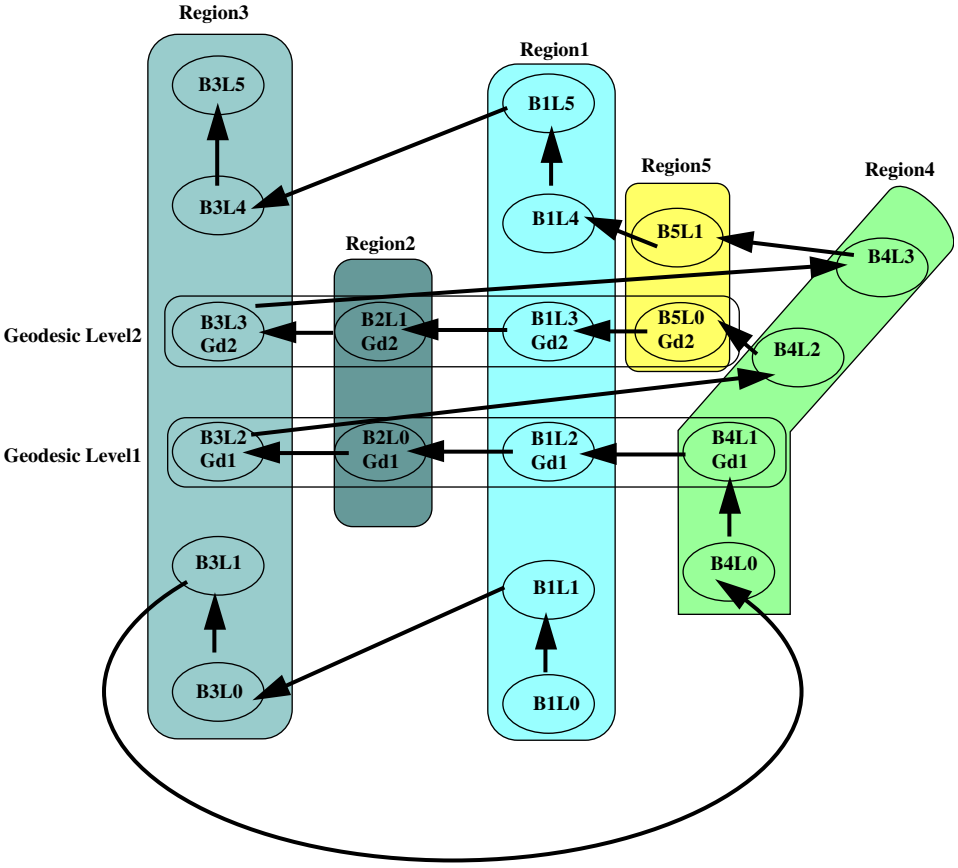

Fig. 4. Establishing geodesic level and process sequence for a solid divided into five subregions.

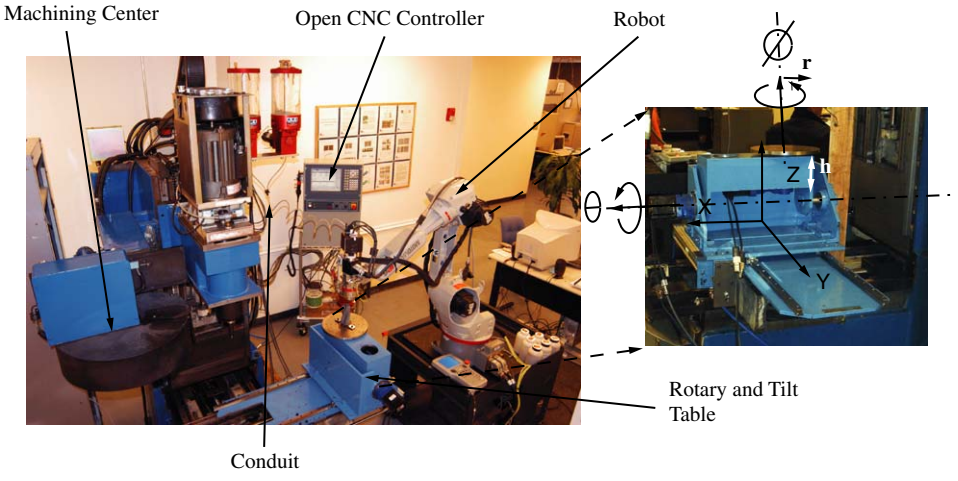

Fig. 5. *MultiFAB*, a multiple axis and machining center.

the dependency of the geometry on the parameters. The rule attributes are derived from the facts that are easy to acquire and can be expressed with simple atomic sentence expressions. For example, the fact that the orientation vector of a sub-region R_p of a solid S, defined by the orientation vector is expressed as the tuple $\langle 0\hat{i}, \frac{1}{\sqrt{2}}\hat{j}, \frac{1}{\sqrt{2}}\hat{k}\rangle$ is expressed by

$$\mathrm{OV}\left(\mathrm{SR}(S, R_p), \mathrm{Vector}\left(\left\langle 0, \frac{1}{\sqrt{2}}, \frac{1}{\sqrt{2}}\right\rangle\right)\right). \tag{4}$$

Similarly the fact, that a layer L_m which belongs to a subregion R_p of a solid S and has the sequence-number 16 is

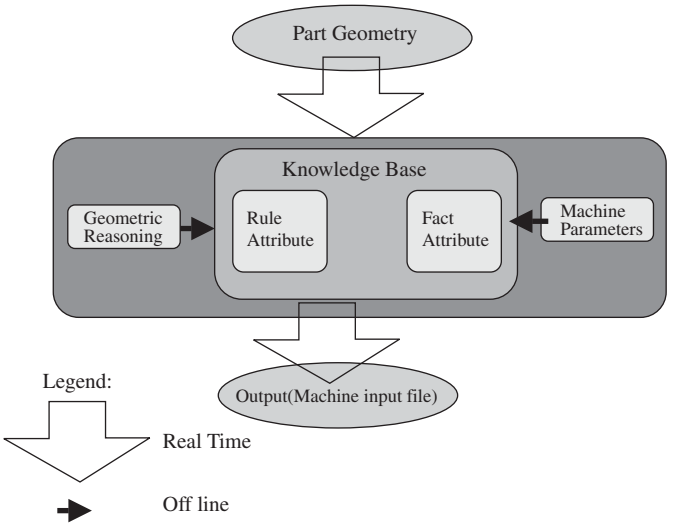

Fig. 6. A schematic diagram of the process planner/expert system.

expressed by

$$\mathrm{SN}(L_m, 16) \wedge \mathrm{BT}(\mathrm{SR}(S, R_p), L_m). \tag{5}$$

The process planning for every solid is considered as a distinct problem; therefore, the above equations can be simplified by ignoring the exclusive representation for solid. The equations, therefore, are modified to

$$\mathrm{OV}\left(R_p, \mathrm{Vector}\left(\left\langle 0, \frac{1}{\sqrt{2}}, \frac{1}{\sqrt{2}}\right\rangle\right)\right) \tag{6}$$

and

$$\mathrm{SN}(L_m, 16) \wedge \mathrm{BT}(R_p, L_m). \tag{7}$$

In the above atomic sentences, the R_p, 16, L_m, $\langle 0, \frac{1}{\sqrt{2}}, \frac{1}{\sqrt{2}}\rangle$ are the constants and predicate arguments; whereas, OV (orientation vector), Vector, SN (sequence number), SR (sub-region), and BT (belongs to) are the functions. Note that R_p, L_m are the integers corresponding to the region number and the layer number of a particular region, respectively.

The derivation of the machine inputs directly from the part geometry requires a suitable representation of the part geometry, the process parameters, and the relationship between the process parameters and the part geometry. However, much complexity is involved with the representation due to an intrinsic requirement of the procedural and non-procedural knowledge [20]. There exists, however, a hierarchical and structured relationship between the part geometry and the corresponding processes steps. The object description and relationships are captured by a set of well defined ontology and a symantic structure that is, in essence, predicate calculus. More complex expressions are expressed by introducing the connectives and the quantifiers. For example, the sentence "if a subregion has the skeletal vector $\langle 0, 0, 1\rangle$, then it is vertical" is expressed as

$$\mathrm{OV}(R, \mathrm{Vector}(\langle 0, 0, 1\rangle)) \Rightarrow \mathrm{Vertical}(R). \tag{8}$$

Similarly "a vertical subregion does not require support" is expressed as

$$\forall R, \mathrm{Vertical}(R) \Rightarrow \neg\mathrm{ReqSupport}(R). \tag{9}$$

A more comprehensive sentence "if the layers from two subregions interfere, then the layers have the same interference-geodesic-level, and are arranged in the order of region number" may be expressed by

$$\begin{aligned}&\forall R_1, R_2\ \ \exists L_1, Sq_1, N_1\ \ \mathrm{SN}(L_1, N_1) \wedge \mathrm{BT}(R_1, L_1)\\ &\quad \wedge \exists L_2, Sq_2, N_2\ \ \mathrm{SN}(L_2, N_2) \wedge \mathrm{BT}(R_2, L_2)\\ &\quad \wedge \mathrm{Interfere}(L_1, L_2) \wedge (R_1 < R_2) \Rightarrow\ \ \exists G\ (\mathrm{GL}(L_1) = G)\\ &\quad \wedge (\mathrm{GL}(L_2) = G) \wedge (Sq_1 < Sq_2).\end{aligned} \tag{10}$$

Note that the interference-geodesic-level-order is the order of build assigned to all the layers at the same interference-geodesic-level. GL is the geodesic function level. Next, further simplification is done by using the notion of skolemization. Skolemization of a formula in essence refers to the elimination of its existential quantifier to produce a formula that is equisatisfiable to the original. The procedure for skolemization is as follows:

1. For positive positions $\exists x f(x) \to f(g(y_1, y_2, \ldots, y_n))$.
2. For negative positions $\forall x f(x) \to f(g(y_1, y_2, \ldots, y_n))$.

The function $g(x)$ is called *Skolem function* and the variables $y_1, y_2, \ldots, y_n$ are *Skolem variables* [21]. The simplification to obtain a quantifier-free formula is done using the propositional simplification laws and applying the following steps:

Step 1: Eliminate the implications.

Step 2: Distribute the negations over the logical operators such that the form includes atomic sentences connected by the logicals.

Step 3: Eliminate the existential quantifiers by introducing skolem constants. For the existential quantifiers within the scope of a universal quantifier, create a skolem function that takes the variable names in the scope of an existential quantifier as a parameter.

Step 4: Drop the universal quantifiers.

Step 5: Restore the implication.

Step 6: Transform the resulting expression into a set of equivalent clausal expressions.

Expression 7 can be transformed as described below:

$$\begin{aligned}&\neg\ \forall R_1, R_2\ \ \exists L_1, Sq_1, N_1\ \ \mathrm{SN}(L_1, N_1) \wedge \mathrm{BT}(R_1, L_1)\\ &\quad \wedge \exists L_2, Sq_2, N_2\ \ \mathrm{SN}(L_2, N_2) \wedge \mathrm{BT}(R_2, L_2)\\ &\quad \wedge \mathrm{Interfere}(L_1, L_2) \wedge (R_1 < R_2)\\ &\quad \vee \exists G\ (\mathrm{GL}(L_1) = G) \wedge (\mathrm{GL}(L_2) = G) \wedge (Sq_1 < Sq_2),\end{aligned} \tag{11}$$

$$\begin{aligned}&\exists R_1, R_2\ \forall L_1, Sq_1, N_1\ \ \neg\mathrm{SN}(L_1, N_1) \vee \neg\mathrm{BT}(R_1, L_1)\\ &\quad \vee \exists L_2, Sq_2, N_2\ \ \neg\mathrm{SN}(L_2, N_2) \vee \neg\mathrm{BT}(R_2, L_2)\\ &\quad \vee \neg\mathrm{Interfere}(L_1, L_2) \vee \neg(R_1 < R_2)\\ &\quad \vee\ \ \exists G\ (\mathrm{GL}(L_1) = G) \wedge (\mathrm{GL}(L_2) = G) \wedge (Sq_1 < Sq_2),\end{aligned} \tag{12}$$

$$\forall L_1, Sq_1, N_1 \ \neg \mathrm{SN}(L_1, N_1) \vee \neg \mathrm{BT}(R_1, L_1) \vee \neg \mathrm{SN}(L_2, N_2) \vee \neg \mathrm{BT}(R_2, L_2) \vee \neg \mathrm{Interfere}(L_1, L_2) \vee \neg(R_1 < R_2) \vee (\mathrm{GL}(L_1) = G) \wedge (\mathrm{GL}(L_2) = G) \wedge (Sq_1 < Sq_2), \quad (13)$$

$$\mathrm{SN}(L_1, N_1) \wedge \mathrm{BT}(R_1, L_1) \wedge \mathrm{SN}(L_2, N_2) \wedge \mathrm{BT}(R_2, L_2) \wedge \mathrm{Interfere}(L_1, L_2) \wedge (R_1 < R_2) \Rightarrow (\mathrm{GL}(L_1) = G) \wedge (\mathrm{GL}(L_2) = G) \wedge (Sq_1 < Sq_2). \quad (14)$$

The Interfere is an essential function; whereas, Layer and SeqNum are skolem functions with the return value of the region corresponding and the sequence number of the interfering layers where R_1, R_2, L_1, L_2, Sq_1 and Sq_2 are the variables.

A close observation of the formulae reveals that the expressions can be represented by a semantic network, in essence conceptual graphs such that various relationships between the objects and the situations (nodes) can be captured by directional links representing the association between the pair of objects. The semantic network [22] forms a knowledge base to mimic the deposition system that includes:

1. Manipulatability.
2. Interaction of the system and substrate.
3. Kinematics.
4. Geometry.
5. Layer scheduling.

The knowledge base is a set of user-defined "if–then" rules of form if $(A_1, A_2, \ldots, A_n)$ then $(\mathrm{Action}_1, \mathrm{Action}_2, \ldots, \mathrm{Action}_n)$ where A_i $(i = 1, 2, \ldots, n)$ are the facts that determine the applicability of rules. An schematic diagram of the expert system that forms the basis for the semantic network is described in Fig. 6.

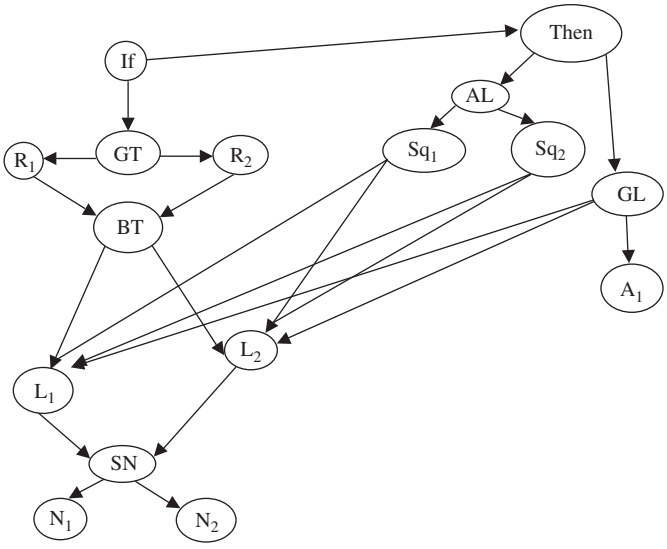

Fig. 7. The semantic tree structure for Expression 10.

The complete set of rules for the process planning can be arranged suitably to generate a more complex and larger semantic tree. For example, the semantic network described in Fig. 7 describes the conclusions drawn from the relations expressed by Expression 10. The landmarks in the Fig. 7 are self explanatory. The implementation of the semantic network as a rule-based framework is done using C++. The framework for Expression 10 captured in Fig. 7 is given by the following pseudocode:

```
(rule   (if interfere          ((L1, R1)(L2, R2) Status)
        (STATUS TRUE)
        (Then                  (Assign (L1 GD)G)
                               (Assign (L2 GD)G)
                               (if LessThan (R1 R2) Status)
                               (STATUS TRUE)
                               (Then (Assign (Sq1) Num)
                               (Assign (Sq2) Num + 1))))).
```

The overall process planning therefore can be captured as expressed by a "*if–then*" based frame following the template:

```
(rules  (rules1  (rule1 (if ···)  (then ···))
                 (rule2 (if ···)  (then ···))
                        ···)
        (rules2  (rule1 (if ···)  (then ···))
                        ···)
                                  ·····)).
```

One of the drawbacks associated with the above approach, that must be addressed includes purely forward reasoning for the process planning. However, a through selection of the knowledge based and suitable arrangement of the objects and the rules allows for a smooth process planning.

6. The rule base and the plan expressed in first order logic

This section elaborates the rule base and the fact base for process planning of the LBMDMD process. The component attributes of a unit vector $\vec{e_1}, \vec{e_2}, \vec{e_3}$, are expressed as a tuple $\langle e_1, e_2, e_3 \rangle$. The slice is expressed as a tuple L_n, R_n, Gd_n, Sq_n, of its attribute that includes layer number L_n, the sub-region number R_n the slice belongs to, the geodesic interference level number Gd_n of the slice and the sequence number Sq_n. All the slices do not necessarily interfere; therefore, the initial geodesic interference level number assigned to all the layers is zero. As the interference between the layers is identified, the geodesic level number is assigned to the layer. The initially assigned sequence number for each layer is zero as well. The Rules 1–4 establish the layer sequence; whereas, the rest of the rules establish the desired orientation of the layer for the deposition. While a more appropriate representation of

the layer and vectors is expressed by Layer ($\langle L_n, R_n, Gd_n, Sq_n\rangle$) and vector($\langle e_1, e_2, e_3\rangle$). The following formulae do not exclusively classify the tuples.

6.1. Rule 1

Every layer has a orientation vector:

$$\forall\langle L_n, R_n, Gd_n, Sq_n\rangle, \exists\langle e_1, e_2, e_3\rangle \mathrm{OV}(\langle L_n, R_n, Gd_n, Sq_n\rangle, \langle e_1, e_2, e_3\rangle). \quad (15)$$

6.2. Rule 2

Any two layers that interfere are assigned the same geodesic interference level.

$$\forall\langle L_1, R_1, Gd_1, Sq_1\rangle \ \forall\langle L_2, R_2, Gd_2, Sq_2\rangle \ \mathrm{Interfere}(\langle L_1, R_1, Gd_1, Sq_1\rangle, \langle L_2, R_2, Gd_2, Sq_2\rangle) \Rightarrow \exists Gd_x \ (Gd_1 = Gd_x) \wedge (Gd_2 = Gd_x). \quad (16)$$

6.3. Rule 3

For a geodesic interference level, the sequence number assigned to the layers is in the same order as the region number of the layers.

$$\exists Gd_x \forall\langle L_1, R_1, Gd_x, Sq_1\rangle \ \forall\langle L_2, R_2, Gd_x, Sq_2\rangle R_1 < R_2 \Rightarrow \exists Sq_a, Sq_b (Sq_a < Sq_b) \wedge \mathrm{Assign}(Sq_1, Sq_a) \wedge \mathrm{Assign}(Sq_2, Sq_b). \quad (17)$$

6.4. Rule 4

For the same subregion of a solid, the sequence number assigned to the layers is in same order as the layer number. However, the precedence order of the geodesic interference level number must be ensured.

$$\exists R_x \forall\langle L_1, R_x, Gd_x, Sq_1\rangle \ \forall\langle L_2, R_x, Gd_x, Sq_2\rangle((Gd_1 < Gd_2) \vee (Gd_1 = Gd_2)) \wedge (L_1 < L_2) \Rightarrow (Sq_1 < Sq_2). \quad (18)$$

Note that the equality of the geodesic interference level of two layers in the same region holds true only for the cases when it is zero; i.e. they do not interfere with any other layer.

6.5. Rule 5

The layer with the orientation vector 0, 0, 1 has a vertical orientation.

$$\forall\langle L_1, R_1, Gd_1, Sq_1\rangle \forall\langle e_1, e_2, e_3\rangle \mathrm{OV}(\langle L_1, R_1, Gd_1, Sq_1\rangle, \langle e_1, e_2, e_3\rangle) \wedge (e_1 = 0) \wedge (e_2 = 0) \wedge (e_3 = 1) \Rightarrow \mathrm{Vertical}(\langle L_1, R_1, Gd_1, Sq_1\rangle). \quad (19)$$

6.6. Rule 6

For every layer that is not vertical, primary, and secondary orientation angles θ and ϕ expressed as an ordered tuple $\langle\theta, \phi\rangle$ can be determined by the mathematical manipulation of the components of the orientation vector (details in the formula below).

$$\forall\langle L_1, R_1, Gd_1, Sq_1\rangle \neg \mathrm{Vertical}(\langle L_1, R_1, Gd_1, Sq_1\rangle) \Rightarrow \exists\langle\theta, \phi\rangle \mathrm{OV}(\langle L_n, R_n, Gd_n, Sq_n\rangle\langle e_1, e_2, e_3\rangle) \wedge (\theta = \mathrm{ArcTan}(e_2/e_3)) \wedge (\phi = \mathrm{ArcTan}(e_1/e_2)). \quad (20)$$

6.7. Rule 7

The reorientation of a layer from any arbitrary configuration to the vertical configuration is expressed by the following action schemata:

$$\begin{aligned}&\mathrm{RotateOperation}(\mathrm{ACTION}: \mathrm{RotateLayer}(\langle L_1, R_1, Gd_1, Sq_1\rangle)\\ &\mathrm{PRECOND}: \neg\mathrm{Vertical}(\langle L_1, R_1, Gd_1, Sq_1\rangle)\\ &\mathrm{EFFECT}: \mathrm{Vertical}(\langle L_1, R_1, Gd_1, Sq_1\rangle)).\end{aligned} \quad (21)$$

6.8. Rule 8

The rotations by (θ) and (ϕ) introduce a displacement Δx, Δy, Δz (Note: the r and h are explained in Fig. 5):

$$\begin{aligned}\Delta x &= r\cos\theta\cos\phi + h\sin\phi,\\ \Delta y &= r\sin\theta,\\ \Delta z &= r\cos\theta\sin\phi - h\cos\phi,\end{aligned} \quad (22)$$

when expressed as the action scheme:

$$\begin{aligned}&\mathrm{RotateOperation}(\mathrm{ACTION}: \mathrm{Rotate}(\langle L_1, R_1, Gd_1, Sq_1\rangle, \langle\theta, \phi\rangle)\\ &\mathrm{PRECOND}: (\Delta x = 0) \wedge (\Delta x = 0) \wedge (\Delta x = 0)\\ &\mathrm{EFFECT}: (\Delta x = r\cos\theta\cos\phi + h\sin\phi) \wedge\\ &(\Delta y = r\sin\theta) \wedge\\ &(\Delta z = r\cos\theta\sin\phi - h\cos\phi)).\end{aligned} \quad (23)$$

6.9. Rule 9

For a slice that is not vertical, in order to get a vertical orientation the spatial manipulation of the substrate, use the following order:

1. Rotate θ.
2. Rotate ϕ.
3. Translate Δx.
4. Translate Δy.
5. Translate Δz.

The schematic for the action is expressed as:

SchemeForVerticalOrientation(
STEPS: {
RotateByTheta(ACTION: RotateBy($\langle L_1, R_1, Gd_1, Sq_1\rangle, \theta$)
PRECOND: $(\Delta x = 0) \wedge (\Delta x = 0) \wedge (\Delta x = 0) \wedge (\theta \neq 0)$
$\wedge (\phi \neq 0)$
EFFECT: $(\Delta x \neq 0) \wedge (\Delta y \neq 0) \wedge (\Delta z \neq 0) \wedge (\theta = 0)$
$\wedge (\phi \neq 0))$

RotateByPhi(ACTION: RotateBy($\langle L_1, R_1, Gd_1, Sq_1\rangle, \phi$)
PRECOND: $(\Delta x \neq 0) \wedge (\Delta y \neq 0) \wedge (\Delta z \neq 0) \wedge (\theta = 0)$
$\wedge (\phi \neq 0)$
EFFECT: $(\Delta x \neq 0) \wedge (\Delta y \neq 0) \wedge (\Delta z \neq 0) \wedge (\theta = 0)$
$\wedge (\phi = 0))$

MoveAlong$X$(ACTION: MoveBy($\langle L_1, R_1, Gd_1, Sq_1\rangle, \Delta x$)
PRECOND: $(\Delta x \neq 0) \wedge (\Delta y \neq 0) \wedge (\Delta z \neq 0) \wedge (\theta = 0)$
$\wedge (\phi = 0)$
EFFECT: $(\Delta x = 0) \wedge (\Delta y \neq 0) \wedge (\Delta z \neq 0) \wedge (\theta = 0)$
$\wedge (\phi = 0))$

MoveAlong$Y$(ACTION: MoveBy($\langle L_1, R_1, Gd_1, Sq_1\rangle, \Delta y$)
PRECOND: $(\Delta x = 0) \wedge (\Delta y \neq 0) \wedge (\Delta z \neq 0) \wedge (\theta = 0)$
$\wedge (\phi = 0)$
EFFECT: $(\Delta x = 0) \wedge (\Delta y = 0) \wedge (\Delta z \neq 0) \wedge (\theta = 0)$
$\wedge (\phi = 0))$

MoveAlong$Z$(ACTION: MoveBy($\langle L_1, R_1, Gd_1, Sq_1\rangle, \Delta z$)
PRECOND: $(\Delta x = 0) \wedge (\Delta y = 0) \wedge (\Delta z \neq 0) \wedge (\theta = 0)$
$\wedge (\phi = 0)$
EFFECT: $(\Delta x = 0) \wedge (\Delta y = 0) \wedge (\Delta z = 0) \wedge (\theta = 0)$
$\wedge (\phi = 0))\}$

ORDER: {RotateByTheta $\prec$ RotateByPhi $\prec$ MoveAlong$X$
$\prec$ MoveAlong$Y$ $\prec$ MoveAlong$Z$}). (24)

The total number of steps is reduced by suitable ordering. Since the reorientation of a layer involves a number of readjustment steps, a reduction in the number of reorientation is desired from an optimal algorithm.

7. Data structure and the query mechanism

The organization of data input is guided by the query structure. The query structure maintains the compatibility with the input data format and reduces the total computation time. An object oriented approach is followed towards the implementation. The main classes used in the implementation are the *region* and *slice* classes. The primary attributes of the *region* class are *region number*, *region vector*, *slice list*, *location of base* and *list of intersecting solids*. Corresponding primary functions of the *region* class are *slice*, *geodesic query* and *fabrication number*. Similarly the primary attributes of the *slice* class include *region number*, *slice number*, *geodesic number*, *slice vector*, *fabrication number*, *base location*, *intersection solid* and *path curve* whereas the main functions are *orientation query*, *path curve*, and *location transform*.

The variables associated with the region include the region number, the vector associated with the region, the list of the slices, the location of the region, and the list of intersection solids. The list of intersection solids is obtained by intersecting the C-space subregions in order to investigate the possible collision. The inputs provided by the geometry of the intersection solid reduces the total computation by reducing the list of slices towards the query for assigning the geodesic level number.

Similarly, the slice class maintains the list of slices for a region. The associated variables include the region number, the slice number, the geodesic order number, the vector, the number for the order of fabrication, the location, the path curve for the deposition, and the list of intersecting solids that overlap with the slice. Also associated are the functions for the transform for the vertical orientation of the slice and the function for the path generation curve for the slice.

The query order followed and the outcome is given as:

- InterferenceQuery(R1, R2). Identifies the interfering regions and attributes the interfering solid to the interfering regions.
- SliceQuery1(L,S). Identifies the colliding layers.
- SliceQuery2(L1,L2). Identifies the interfering layers and assigns the geodesic number.
- SliceQuery3(L). Assigns the final order of the lists.
- SliceQuery4(L). Determines the primary and secondary angle and the spatial adjustments for the vertical orientation of the layers.

The algorithm used to generate the final inputs for the reorientation of the slices is expressed as following:

function ProcessPlanningSteps (Sequential-tuple-of-Layers)
return machine-input-file
for **i** $\leftarrow$ 1 to **maxLayers**
if ($\theta \geqslant 0$ or $\phi \geqslant 0$)
determine($\Delta x, \Delta y, \Delta z$)
rotate(θ)
rotate(ϕ)
translate(Δx)
translate(Δy)
translate(Δz)
for **j** $\leftarrow$ 1 to **maxRegion**
update(θ and ϕ)

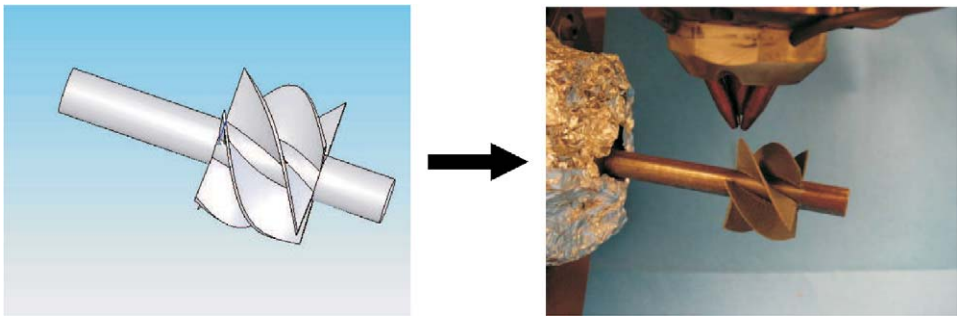

Fig. 8. The computer model and the part fabricated by multi-axis deposition.

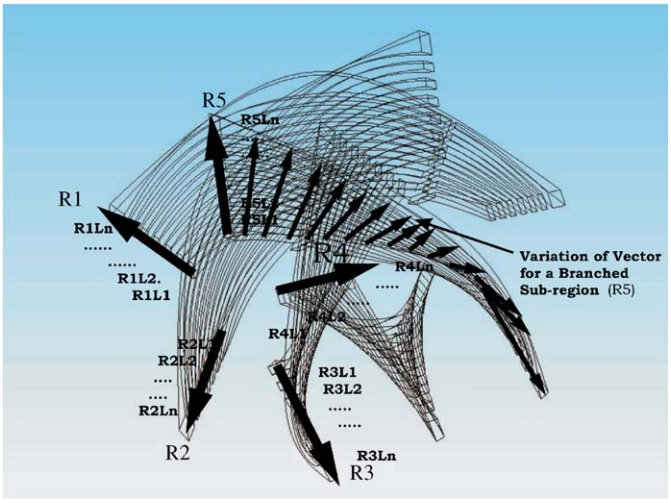

Fig. 9. The slicing scheme and variation of the vectors for a branched-subregion of the model described in Fig. 8.

Table 1
Geometric parameters for the scheme described in Fig. 9

Region	Orientation vector of the skeleton	Rotation angle of the platform (in degrees)	Layer: $R_i \equiv i$th region, $L_i \equiv i$th region
Region 1	$-0.95\hat{x} + 0.31\hat{y}$	162	$R1L1, R1L2\ldots$
Region 2	$-0.59\hat{x} - 0.81\hat{y}$	−126	$R2L1, R2L2\ldots$
Region 3	$0.59\hat{x} - 0.81\hat{y}$	−54	$R3L1, R3L2\ldots$
Region 4	$0.95\hat{x} + 0.31\hat{y}$	18	$R4L1, R4L2\ldots$
Region 5	$\hat{y}$	90	$R5L1, R5L2\ldots$

8. Experimental verification

The implementation of the method and the geometrical queries are based on the API kernel provided by the ACIS. Fig. 8 describes a highly complex branched geometry fabricated using the experimental setup. The part geometry consists of twisted thin wall structures mounted at equal intervals on a cylinder. The part has overhanging regions. Fabrication of the part using the popular $2\frac{1}{2}$ method will need support structures for the overhanging regions, thus introducing the requirement for post-processing steps.

Due to the complexity of the geometry, the part is described by a large set of direction vectors, as described in Fig. 9. However, the suitable relative motion of the substrate and the metal deposition head simplify the number of inputs and allow the fabrication of the part without support structures. The part slicing is done as described in Fig. 9. A cylindrical substrate rotates about its axis; whereas, the metal deposition head moves along the axial direction of the cylinder such that the metal is deposited on the lateral surface. Note that the number of layers shown in Fig. 9 is smaller than the actual number of layers. Correspondingly, the layer thickness shown is more than the actual layer thickness for the visualization purpose.

The overhanging wall features appear at an angle of 72°. The part is decomposed into five exclusive regions based on the support requirement. The process parameters are summarized in Table 1. The direct fabrication of the wall leads to the interference of the metal deposition head with the adjacent deposited wall; therefore, the order followed for the layers is: $L1R1 \rightarrow L1R2\ldots L1R5 \rightarrow L2R1 \rightarrow L2R2\ldots L2R5 \rightarrow LnR1 \rightarrow LnR2\ldots LnR5$. The final part is shown in Fig. 8. Apart from the geometry, heat-transfer is another factor considered for a smooth deposition; however, a discussion of the heat-transfer related issues is beyond the scope of this research.

Fig. 10 shows a hollow spiral that is more complex. The axial pitch and the radius of the spiral vary over time. The thickness of the wall is 1 mm; whereas, the cross-section of the swept area is 10 mm × 10 mm. The convoluted non-linear geometry of the helix, impose the requirement of a continuous variation of the metal deposition direction vector. However, for the generation of the input data for the machine, the height of every cylinder is of the order of the layer (0.4 mm). Due to the finite size of the metal deposition head, the diameter and the pitch of the helix are limited by the dimensions of the metal deposition head. The relative location, the orientation, and the subsequent transform required are characterized by the desired geometry of the spiral. The decomposition of the CAD model of the spiral is done in such a way that every slice corresponds to a different region.

Fig. 10 also illustrates a large view of the slice geometry representation used for the process planning. The total

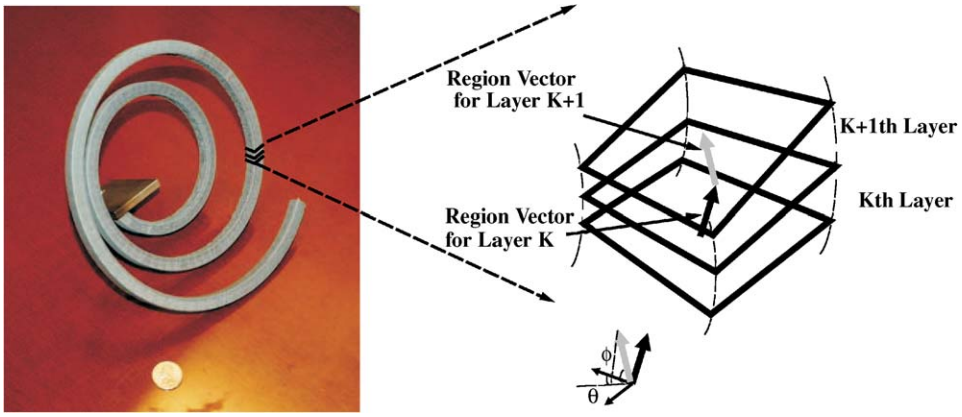

Fig. 10. A hollow spiral fabricated by multi-axis deposition.

time required to fabricate a part includes the time required for the metal deposition and the time required for the reorientation of the buildup or part. While the metal deposition speed can be constant for most of the structures, the time required for the part orientation plays a critical role.

9. Conclusions and future work

The multi-directional metal deposition by LBDMD allows the fabrication of a near-net shape part fabrication without a support requirement. The principles of first order logic and planning have been employed to capture the intent of planning steps. The first order logic expressions are then simplified into a format suitable for the implementation using a coding scheme based on an "if–then" rule knowledge base. The experiments performed for simple geometries depict satisfactory results. One of the limitations of the algorithm is that it primarily relies on the forward search; therefore, it cannot take into account the errors introduced. The future work seeks to include the model for the error introduction and error propagation, and a backward search in the algorithm.

Acknowledgements

The authors gratefully acknowledge the support for this work by the National Science Foundation under the Grant no. DMI-0320663. Authors would also like to acknowledge the help extended towards the preparation of experimental setup by Mr. M. Valant, Research Engineer and Mr. Srdja Zekovic Graduate student at RCAM.

References

[1] S.M. Weiss, C.A. Kulikowski, A Practical Guide to Designing Expert Systems, Rowman & Littlefield, Totowa, NJ, USA, 1984.
[2] J. Stein, On the solution of layout problems in multiagent systems: a preliminary report, in: Proceedings of the 10th Conference on Artificial Intelligence for Applications, San Antonio, TX, 1994, pp. 2–8.
[3] S. Fujita, M. Otsubo, M. Watanabe, An intelligent control shell for cad tools, in: Proceedings of the 10th Conference on Artificial Intelligence for Applications, San Antonio, TX, 1994, pp. 16–22.
[4] R.G. Arbon, P.R. Riethmeier, G.G. Mally, T.W. Osborne, R.L. Tharrett, Auto-mps: an automated master production scheduling system for large volume manufacturing, in: Proceedings of the 10th Conference on Artificial Intelligence for Applications, San Antonio, TX, 1994, pp. 26–32.
[5] D.M. Gaines, W.C. Regli, Special issue: new artificial intelligence paradigms for manufacturing, Artificial Intelligence for Engineering Design, Analysis and Manufacturing 17 (3) (2003) 171.
[6] A. Famili, P. Turney, Application of machine learning to industrial planning and decision making, in: A.F. Famili, D.S. Nau, S.H. Kim (Eds.), Artificial Intelligence Applications in Manufacturing, AAAI Press, Menlo Park, CA, 1992, pp. 1–16.
[7] G. Zhang, S.C. Lu, An expert system approach for economic evaluation of machining operation planning, in: A.F. Famili, D.S. Nau, S.H. Kim (Eds.), Artificial Intelligence Applications in Manufacturing, AAAI Press, Menlo Park, CA, 1992, pp. 133–156.
[8] P. Singh, D. Dutta, Multi-direction slicing for layered manufacturing, Journal of Computing and Information Science and Engineering 2 (2001) 129–142.
[9] J. Zhang, J. Ruan, F.W. Liou, Process planning for a five-axis hybrid rapid manufacturing process, in: Proceedings of the 11th Solid Freeform Fabrication Symposium, Austin, TX, 2000.
[10] P. Singh, Y. Moon, D. Dutta, S. Kota, Design of a customized multi-directional layered deposition system based on part geometry, in: Proceedings of the 14th Solid Freeform Fabrication Symposium, Austin, TX, 2003.
[11] S. McMains, Double sided layered manufacturing, in: Proceedings of the Japan–USA Symposium on Flexible Automation, Hiroshima, Japan, 2002, pp. 269–272.
[12] R. Dwivedi, R. Kovacevic, Process planning for multi-directional laser-based direct metal deposition, Proceedings of the Institution of Mechanical Engineers, Journal of Mechanical Engineering Science C219 (2005) 695–707.
[13] J.A. Bærentzen, M. Sramek, N.J. Christensen, A morphological approach to the voxelization of solids, in: Winter School of Computer Graphics (WSCG) 2000, vol. 1, University of West Bohemia, Plzen, Czech Republic, 2000, pp. 44–51.
[14] E. Ferley, M.-P. Cani, D. Attali, Skeletal reconstruction of branching shapes, Computer Graphics Forum 16 (5) (1997) 283–293.
[15] T. Culver, Computing the medial axis of a polyhedron reliably and efficiently, Ph.D. Thesis, University of North Carolina, Chapel Hill, 2000 (director–Dinesh Manocha).
[16] D. Attali, P. Bertolino, A. Montanvert, Using polyballs to approximate shapes and skeletons, in: Pattern Recognition, Proceedings of the CVIP, 1994, pp. 626–628.

[17] N. Gagvani, D. Kenchammana-Hosekote, D. Silver, Volume animation using the skeleton tree, in: VVS '98: Proceedings of the 1998 IEEE Symposium on Volume Visualization, ACM Press, New York, NY, USA, 1998, pp. 47–53.
[18] R. Dwivedi, R. Kovacevic, Automated torch path planning using polygon subdivision, SME Journal of Manufacturing Systems 23 (4) (2004) 267–281.
[19] R. Kovacevic, System and method for fabricating or repairing a part, Accepted Patent Application No. 10/649,925 (2003).
[20] L. Congxin, H. Shuhuai, W. Yungan, An Expert System for Designing Hydraulic Schemes, Springer, Berlin, 1991, pp. 391–413 (chapter 16).
[21] E. Clarke, X. Zhao, Analytica—a theorem prover in mathematica, in: Automated Deduction-CADE-II, 11th International Conference on Automated Deduction, Saratoga Springs, New York, 1992, pp. 761–763 URL <citeseer.csail.mit.edu/clarke93analytica.html>.
[22] S. Russell, P. Norvig, Artificial Intelligence: A Modern Approach, Prentice-Hall, Englewood Cliffs, NJ, 1995.